Extended Hauser-Feshbach method for statistical binary decay of light-mass systems

T. Matsuse,* C. Beck, R. Nouicer, and D. Mahboub
Centre de Recherches Nucléaires, Institut National de Physique Nucléaire et de Physique des Particules–Centre National de la Recherche Scientifique/Université Louis Pasteur, B.P. 28, F-67037 Strasbourg Cedex 2, France
(Received 21 November 1996)

An extended Hauser-Feshbach method (EHFM) is developed for *light* heavy-ion fusion reactions in order to provide a detailed analysis of all the possible decay channels by including explicitly the fusion-fission phase space in the description of the cascade chain. The mass-asymmetric fission component is considered as a complex-fragment binary decay which can be treated in the same way as the light-particle evaporation from the compound nucleus in statistical-model calculations. The method of the phase-space integrations for the binary decay is an extension of the usual Hauser-Feshbach formalism to be applied to the mass-symmetric fission part. The EHFM calculations include ground-state binding energies and discrete levels in the low-excitation-energy regions which are essential for an accurate evaluation of the phase-space integrations of the complex-fragment emission (fission). In the present calculations, the EHFM is applied to the first-chance binary decay by assuming that the second-chance fission decay is negligible. In a similar manner to the description of the fusion-evaporation process, the usual cascade calculation of light-particle emission from the highly excited complex fragments is applied. This complete calculation is then defined as EHFM+CASCADE. Calculated quantities such as charge-, mass, and kinetic-energy distributions are compared with inclusive and/or exclusive data for the $^{32}S+^{24}Mg$ and $^{35}Cl+^{12}C$ reactions which have been selected as typical examples. Finally, the missing charge distributions extracted from exclusive measurements are also successfully compared with the EHFM+CASCADE predictions. [S0556-2813(97)06803-9]

PACS number(s): 24.60.Dr, 25.70.Jj, 25.70.Gh, 25.70.Lm

I. INTRODUCTION

For heavy-ion-induced reactions in both the low- and intermediate-energy regimes, the emission of complex fragments [or intermediate-mass fragments (IMF's)] has been considered to be one of the most useful probes for the investigation of the different reaction mechanisms involved in fissionlike phenomena for a wide mass range of nuclear systems [1–8]. It has been shown that for composite systems in the *light* mass region $A_{CN} \leqslant 60$, the fusion-fission (FF) process plays an important role in the compound nucleus (CN) decay [2,7,9–16]. One of the difficulties in this light-mass region is that the fully damped yields of most of the observed binary-decay products are mixed with those of quasielastic as well as deep-inelastic processes and therefore their distinction from FF yields is a rather difficult task for the experimentalist [2,3,7,9,14–16].

For the lighter-mass systems, the nuclear orbiting process induced by a long-lived dinuclear molecular complex, which subsequently binary decays, is among the possible mechanisms of producing complex fragments for which the energy degree of freedom has been fully relaxed [3]. However, the experimental data for the $^{16}O+^{40}Ca$ [2], $^{32}S+^{24}Mg$ [9], $^{35}Cl+^{12}C$ [7], $^{31}P+^{16}O$ [10], and $^{23}Na+^{24}Mg$ [14] reactions have been found to be consistent with an equilibrated CN formation which subsequently binary decays with the emission of complex fragments, i.e., a FF process. The occurrence of FF rather than orbiting in these systems has been the subject of much discussion. This has led to the conclusion that the FF process has to be taken into account when exploring the limitations of the complete fusion process at large angular momenta and high excitation energies [11,14]. Figures 1 and 2 illustrate for the $^{32}S+^{24}Mg$ [9] and $^{35,37}Cl+^{12}C$ [7] reactions, respectively, two typical examples of sets of data which have been selected to be compared with the results of the statistical model developed in the present paper.

The extended Hauser-Feshbach method (EHFM), which has been already presented in several communications [12,17], assumes that the fission probability is taken to be proportional to the available phase space at the scission point. The EHFM corresponds essentially to an extension of the Hauser-Feshbach formalism [18] which treats gamma-ray decay, light-particle evaporation, and complex-fragment emission (or FF) as the possible decay channels in an equivalent way. In this paper we will apply the EHFM to *light* heavy-ion fusion-fission reactions. This is an alternative approach to the transition-state model [11] using the phase space at the saddle point which has provided quite good predictions of the available experimental data [2,9,11,13–16]. Since there are good indications for the validity of the hypothesis that the saddle-point shape almost coincides with the scission-point configurations in the light-mass region, it is expected that the EHFM might also be relevant. Preliminary results of EHFM calculations as performed for the $^{35}Cl+^{12}C$ fission reaction in Ref. [15] are quite conclusive.

This paper is organized as follows. In the next section, the essential points of the EHFM are first presented. After a brief description of the well-known Hauser-Feshbach formalism which is used for the CN light-particle emission, the main characteristics of the formal procedures of the EHFM are

*On leave from the Faculty of Textile Science and Technology, Shinshu University, Ueda, Nagano, 386, Japan, as an Overseas Research Scholar of Japan.

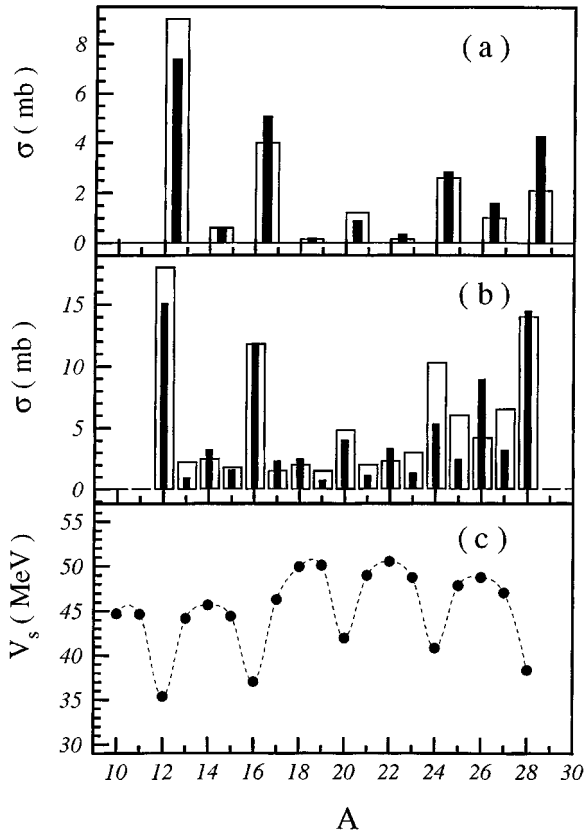

FIG. 1. Comparisons of the experimental mass distributions (open histograms) measured for the $^{32}S+^{24}Mg$ reaction at $E_{lab}=121$ (a) and 142 MeV (b), respectively, with the EHFM +CASCADE calculations (solid histograms). (c) Fragment mass dependence of the lowest scission point barrier height in the set of the binary combination with same mass number but different atomic number for ^{56}Ni. The barrier heights are shown for the case of angular momentum $L=0$ (see text).

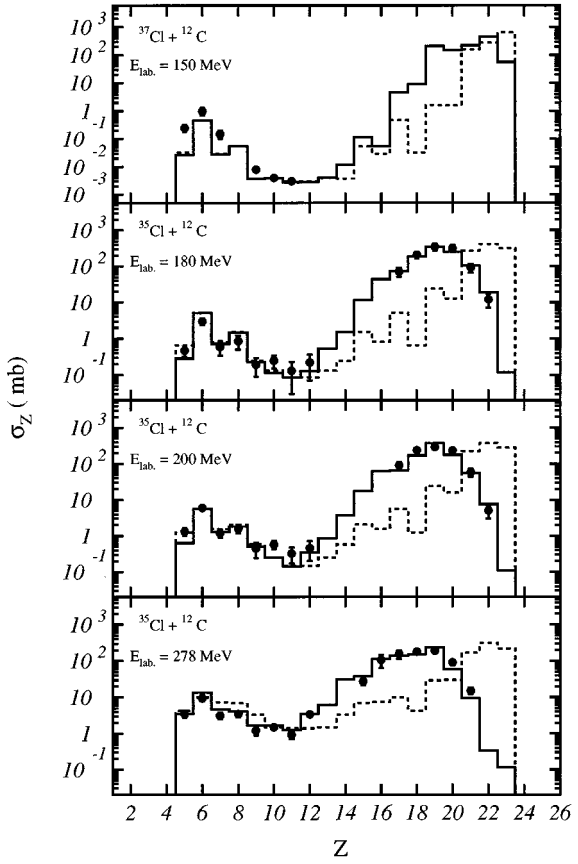

FIG. 2. Experimental charge distributions measured for the $^{35}Cl+^{12}C$ reaction at $E_{lab}=180$, 200, and 278 MeV and for the $^{37}Cl+^{12}C$ reaction at $E_{lab}=150$ MeV. Comparisons with EHFM +CASCADE calculations are shown by solid histograms. The dashed histograms are the results of first-chance EHFM calculations.

described in Sec. III. The complete EHFM+CASCADE calculation is applied for a first-chance fission (or emission of excited complex fragments) followed by their light-particle sequential decays until the resulting products are unable to undergo further decay. This can be considered as a reasonable assumption for light-mass systems as shown previously for a medium light-mass fission reaction [8]. In Sec. IV, the calculated results are shown in the case of a simple parametrization and their applicability to the two selected reactions studied [7,9,15] is discussed (cross sections are plotted in Figs. 1 and 2). Results are summarized and some preliminary conclusions are finally drawn in Sec. V along with a short discussion relative to future directions for systematic investigations and applications of the model to a wider mass range of nuclear systems from the light-mass region to the intermediate-mass region.

II. EXTENDED HAUSER-FESHBACH METHOD

In order to clarify the essential viewpoints of the EFHM calculations, the salient formulas used in the well-known statistical model treatments which are based upon the Hauser-Feshbach formalism [18] to describe the CN light-particle evaporation are presented in next subsection. Given that the statistical model [19], which follows from the assumption of equilibrium, rests on the premise that all open decay channels are, on the average, equally likely to be populated, it was natural to extend its formalism. Although the treatment of light-particle emission and FF is, in principle, inconsistent for heavier nuclear systems, it has been shown that in the case of lighter nuclei (where the fissility parameters are below the Businaro-Gallone point [1]) the asymmetric fission process can be assimilated to the emission of larger fragments [20] which are also known as complex fragments (or IMF's). Light-particle evaporation and FF, which are the two commonly observed CN decay modes, appear to be just two extremes of a more general binary-decay mode involving the entire range of mass asymmetry [20]. The extension of the Hauser-Feshbach method [18] to the complex-fragment emission and/or FF is explained in Sec. II B within the framework of all available phase space. A brief description of the parametrization of the transmission coefficients and its approximations are given in Sec. II C. The complete calculation procedures of EHFM+CASCADE which take into account the sequential emission of light particles and gamma rays from the excited fission (or complex) fragments are finally presented in Sec. III.

A. Hauser-Feshbach method for light-particle evaporation

Most of the commonly used statistical-model codes, such as CASCADE [21], PACE [22], or LILITA [23] which have pro-

vided good predictive results for the evaporation residues (ER) yields measured for a large number of fusion-evaporation reactions, are based on a method proposed by Hauser and Feshbach more than four decades ago [18].

In the Hauser-Feshbach method the cross section $\sigma_J^{(c)}$ for the CN formation and its subsequent statistical decay to channel c whose state is populated at an excitation energy E_x with a total angular momentum J are given by using the decay ratio $R_J^{(c)}$ as follows:

$$\sigma_J^{(c)} = R_J^{(c)} \sigma_J(E_x) \ , \tag{1}$$

where $\sigma_J(E_x)$ is the cross section of the populated compound states. Generally the ratio $R_J^{(c)}$ is determined by the ratio of the partial width $\Gamma_J^{(c)}$ to the total width Γ_J,

$$R_J^{(c)} = \frac{\Gamma_J^{(c)}}{\Gamma_J} \ , \tag{2}$$

where the total width is a sum of all the partial widths of the decaying channels c,

$$\Gamma_J = \sum_c \ \Gamma_J^{(c)} . \tag{3}$$

In the case of light-particle evaporation, the decay channel c includes mainly neutron, proton, α-particle channel and γ-ray emission. In some cases it can be also interesting to include ^{2,3}H, ^{3}He, and Li emissions [21], but their influence is found to be negligible for the reactions studied. In this paper these ^{2,3}H and ^{3}He channels are only included in the calculations in the first-chance decay, whereas the Li channel is included and is considered as a complex-fragment emitted by a binary decay in the phase-space calculation of EHFM as will be explained more in detail in the next subsection.

The partial width $\Gamma_J^{(c)}$ is related to a phase-space integration $P_J^{(c)}$

$$\rho_J(E_x)\Gamma_J^{(c)} = \frac{1}{2\pi} P_J^{(c)} \ , \tag{4}$$

where $\rho_J(E_x)$ is the level density of the compound state. This level density is not so relevant for the calculation of the decay ratio $R_J^{(c)}$ in Eq. (2), but has a real physical meaning for the estimation of a mean lifetime τ_J of the compound states. The mean lifetime τ_J of a compound nucleus is generally evaluated by using the total width Γ_J as follows:

$$\tau_J = \frac{\hbar}{\Gamma_J} . \tag{5}$$

This definition will be of interest in the discussion on the differences between the lifetime of the compound states with the time needed to emit a complex fragment near the scission point.

In the well-known Hauser-Feshbach method [18] used to describe the light-particle emission, the phase-space integration $P_J^{(c)}$ to the channel c is evaluated by the following phase-space integration:

$$P_J^{(c)} = g_c \sum_{(L,I)J} \int \int \rho_I(\epsilon) T_L(E) \delta(\epsilon + E + Q - E_x) d\epsilon dE \ . \tag{6}$$

Here g_c denotes the spin multiplicity of the evaporated particle and $\rho_I(\epsilon)$ is the level density of the residual nucleus with internal excitation energy ϵ and angular momentum I. Here $T_L(E)$ are the transmission coefficients for the evaporated particles as a function of energy E and angular momentum L in the relative motion with the daughter nucleus. We use the transmission coefficients obtained in the optical-model (OM) calculations in which the potential parameters have smooth dependences on the mass number and are standard in the statistical-model calculations [19,21]. The $(L,I)J$ shown in the summation of angular momentum represents the proper angular momentum coupling condition. The energy conservation condition is maintained by $\delta(\epsilon + E + Q - E_x)$ in Eq. (6).

As soon as the excited states of the daughter nucleus are low enough in energy, which is normally the case at the end of the cascade calculations, it is necessary to take into account in the phase-space integrations of the light-particle decay the experimentally known discrete levels of the daughter nucleus near its ground state. As a consequence the phase-space integration $P_J^{(c)}$ becomes a summation of the known discrete levels i of the daughter nucleus, instead of the energy integration with ϵ in Eq. (6),

$$P_J^{(c)} = g_c \sum_i \sum_{(L,I_i)J} \int T_L(E) \delta(\epsilon_i + E + Q - E_x) dE \ , \tag{7}$$

where ϵ_i and spin I_i are the known ith discrete levels of the daughter nucleus which have been taken from recent compilations [24,25]. For the emission of γ rays, we include only the giant dipole resonance (GDR) decay by using the form factor of Ref. [26].

The quantity Q is the usual separation energy for the light-particle evaporation which is defined as

$$Q = B_{\rm GS}(N_{\rm CN}, Z_{\rm CN}) - B_{\rm GS}(N_L, Z_L) - B_{\rm GS}(N_H, Z_H) \ , \tag{8}$$

where $B_{\rm GS}(N_{\rm CN}, Z_{\rm CN})$, $B_{\rm GS}(N_L, Z_L)$, and $B_{\rm GS}(N_H, Z_H)$ are the binding energies of the CN, evaporated particle, and daughter nucleus, respectively. The observed ground-state binding energies given by the data tables [27] for the evaluation of Q values are used. If we include, for example, ^{3}He evaporation in the calculations, it is found to be negligible, in agreement with experiment results, since ^{3}He has a very small binding energy if compared to the α-particle binding energy.

For the evaluation of the level density the Bohr-Mottelson expression [28], which is derived from the Fermi-gas model, has been used,

$$\rho_I(\epsilon) = \frac{1}{12} \left(\frac{a\hbar^2}{2\mathcal{J}} \right)^{3/2} (2I+1) a \frac{e^{2\sqrt{X}}}{X^2} \ , \tag{9}$$

where

$$X = a \left(\epsilon - \frac{\hbar^2}{2\mathcal{J}} I(I+1) - \Delta_{\rm pair} \right) . \tag{10}$$

The $\mathcal{J}$ is the moment of inertia of the daughter nucleus. In this paper we use the well-parametrized moment of inertia of the spherical nucleus shown in Ref. [28],

$$\mathcal{J}=\tfrac{2}{3}AM\langle r\rangle_A^2, \quad \langle r\rangle_A^2=\tfrac{3}{5}(1.12A^{1/3})^2(1+3.84A^{-1/3}) , \tag{11}$$

where M is the nucleon mass and $\langle r\rangle_A^2$ is the mean-square radius of the ground state of the nucleus. For the sake of simplicity, we use a constant level density parameter value. For the calculations we have chosen the value $a=A/8$ which appears to be rather well established both experimentally [19,21,29] and theoretically [30] for the light heavy-ion systems considered in the present study. The pairing energy $\Delta_{\rm pair}$ is given by the empirical value $\Delta_{\rm pair}=12/\sqrt{A}$ as proposed in Ref. [28].

EHFM calculations have been performed for previously studied complete-fusion reactions in the $A_{\rm CN}\approx 30$ [31] and $A_{\rm CN}=56$ [32] mass regions in order to test the predicting capabilities of the present model for the fusion-evaporation residues. Their comparisons with the data [31,32] and with predictions of the evaporation codes CASCADE [21], PACE [22], or LILITA [23] clearly show that first the number of evaporated light particles is correctly predicted by the EHFM and, second, that the results are not too sensitive to the choices of the approximations and of the parameters of the present model.

B. Extension of the Hauser-Feshbach formalism to the binary decay

The objective of the EHFM is to extend the Hauser-Feshbach formalism [18], which has been described previously, to the phase-space integrations of the binary decays of the complex fragments (or the fission decay width) from the compound nucleus. The phase-space integrations for the complex-fragment binary decays consist of four parts which are defined by the four forthcoming equations.

At first we consider the case of binary decays in which the lighter partner of the binary pair is populated in the discrete levels at low energies near the ground state and the heavier one is in higher-excitation-energy states in the continuum region. The phase-space integration $P_J^{(c)}$ for this binary decay is then assumed to be evaluated by the extension of Eq. (6) as follows:

$$P_J^{(c)}=\sum_i \sum_{(I_{L_i},I_H)I} \sum_{(L,I)J} \int\int \rho_{I_H}(\epsilon_H)T_L(E) \times\delta(\epsilon_{L_i}+\epsilon_H+E+Q-E_x)d\epsilon_H dE , \tag{12}$$

where $\rho_{I_H}(\epsilon_H)$ is the Fermi-gas level density of the heavier fragment with excitation energy ϵ_H and angular momentum I_H. Here ϵ_{L_i} and I_{L_i} are the excitation energy and angular momentum of the ith discrete levels of the emitted light fragments. In the present calculation we introduce the known low excited discrete levels [24,25] in the low-energy region of each binary-decay fragment of interest up to the lowest particle decay threshold energy. The calculated results performed without including discrete levels badly reproduce both the yields and the energy distributions which are known to exhibit a structure understood in terms of the statistical population of levels in the fragments [16].

As in the case of light-particle emission, in this paper the level density is calculated by using the moment of inertia spherical nucleus shown in Eq. (11); thus, the deformation effects are not introduced in the level density of both lighter and heavier fragments in the binary decay. This possibility will be investigated in a subsequent publication [33] by including the angular-momentum-dependent terms in the ground-state moment of inertia as proposed recently by Huizenga *et al.* [34].

In a similar manner to light-particle evaporation, E is the energy of the relative motion between the lighter fragment and heavier binary partner, and $T_L(E)$ is the transmission coefficient of the relative motion with a given angular momentum L. As we are trying to extend the framework of the Hauser-Feshbach method of light-particle emission to the case of complex fragments emission, it is more reasonable to introduce the transmission coefficients obtained in the OM calculation for evaluating the transmission coefficients. However, in this study we will use a simplified formula for the transmission coefficient as will be explained in the following subsection. As will be discussed in the Sec. IV, the phase-space integration of Eq. (12) will mainly contribute to the mass-asymmetric binary decay. Phase-space calculations of this kind have already been extended to the study of the emission of complex fragments in the case of the ^{58}Ni+^{58}Ni reaction with quite reasonable success in predicting complex-fragment charge distributions that have been experimentally measured by the Oak Ridge group [6].

Next we apply the above considerations to the case of the light fragments highly excited in the continuum-energy region. Instead of the summation up to the ith discrete levels, the integration in the excitation energy ϵ_L and summation of angular momentum I_L of the light fragment is performed as follows:

$$P_J^{(c)}=\sum_{(I_L,I_H)I} \sum_{(L,I)J} \int\int\int \rho_{I_L}(\epsilon_L)\rho_{I_H}(\epsilon_H)T_L(E) \times\delta(\epsilon_L+\epsilon_H+E+Q-E_x)d\epsilon_L d\epsilon_H dE , \tag{13}$$

where $\rho_{I_L}(\epsilon_L)$ is the Fermi-gas level density of the light fragment. In order to integrate this large phase space a long computational time is necessary. This is, however, the most essential part of the EHFM which is applied to the mass-symmetric part of FF.

The phase-space calculation for the heavier fragment in the low-excitation-energy region with discrete states in a similar manner to Eq. (12) is as follows:

$$P_J^{(c)}=\sum_j \sum_{(I_L,I_{H_j})I} \sum_{(L,I)J} \int\int \rho_{I_L}(\epsilon_L)T_L(E) \times\delta(\epsilon_L+\epsilon_{H_j}+E+Q-E_x)d\epsilon_{L_j} dE , \tag{14}$$

where ϵ_{H_j} and I_{H_j} denote the excitation energy and angular momentum of the jth discrete level of the heavier partner of binary decay.

In the case where the fragments are both excited in the low-energy region, the phase space is evaluated following Eq. (7) which corresponds to the phase-space integration of light-particle evaporation,

$$P_J^{(c)} = \sum_i \sum_j \sum_{(I_{L_i}, I_{H_j})I} \sum_{(L,I)J} \int T_L(E) \times \delta(\epsilon_{L_i} + \epsilon_{H_j} + E + Q - E_x) dE \ . \quad (15)$$

As shown above, the phase-space integration for the complex-fragment binary decays consists of the four parts which are represented in Eqs. (12), (13), (14), and (15). In the actual calculation, in order to avoid any possible overcounting, the continuum-energy integrations for the level density formulas in Eqs. (12), (13), and (14) are performed in the energy region starting from the energy which is higher than the hightest excitation energy of the discrete levels which are introduced in the discrete level summations of Eq. (15). As mentioned previously, the available discrete levels are taken below the lowest separation energy in the neutron, proton, and alpha-particle separations of the fragments. For the evaluation of Q values in these calculations, the observed ground-state binding energies [27] are correctly used as shown in Eq. (8) to keep the energy conservation condition. This effect, which is clearly visible in Fig. 1(c), will be discussed in Sec. IV.

C. Parametrization of the transmission coefficients

As mentioned in the previous subsection, it would be highly desirable to use explicitly the transmission coefficients of the OM calculations as a natural extension of the Hauser-Feshbach method to the case of complex-fragment emission. However, because of the limitations of the computational time needed to perform OM calculations, the transmission coefficients for these phase-space integrations in Eqs. (12), (13), (14), and (15) are evaluated by using the simplified formula

$$T_L(E) = \frac{1}{1 + \exp\{[V(L) - E]/\Delta_s\}} \ , \quad (16)$$

where the parameter Δ_s is the diffuseness parameter in the transmission coefficient formula whose value has been kept equal to 0.5 MeV in this study. This choice is consistent with the larger 1 MeV value which has been recently chosen for the EHFM description of a heavier mass system [8]. As far as we know, the energy dependence of the transmission coefficients obtained by the OM calculation is roughly fitted by the formula (16) and the chosen diffuseness parameter value is comparable to that of OM calculations in light-mass systems in the low-angular-momentum region. For evaluating the transmission coefficients by the OM, the real part has been deduced from fits to the measured elastic scattering cross sections if available. In the case of ^{35}Cl+^{12}C scattering the OM parameter set extracted from the elastic data measured by Djerroud [13] has been used. The imaginary part is modified by the inclusion of short-range and sharp diffuseness in order to reproduce the energy dependence of measured fusion cross sections for light-mass systems in the so-called first regime of fusion just above the Coulomb barrier. Of course the diffuseness for larger angular momenta in OM calculations becomes much larger with increasing angular momentum. We use the diffuseness parameter which is independent of the angular momentum in this study. The calculations using the transmission coefficients of the OM calculations will be discussed in a forthcoming paper [33].

In order to simplify the discussions of the calculated results which will be given in this paper, we have adopted the simple parametrization of the barrier height $V(L)$ at the scission point between complex fragments which has been assumed in the case of the ^{35}Cl+^{12}C FF reaction [13] to be

$$V(L) = V_{\rm Coul} + \frac{\hbar^2}{2\mu_f R_s^2} L(L+1) \ , \quad (17)$$

where μ_f is the reduced mass of the decaying complex fragments. The scission point R_s is estimated by using the radius $R_L = r_s A_L^{1/3}$ and $R_H = r_s A_H^{1/3}$ of the two fragments of mass number A_L and A_H including diffuse-surface effects with a neck length parameter (or separation distance) d,

$$R_s = R_L + R_H + d \ , \quad (18)$$

and the $V_{\rm Coul}$ is calculated by the simple formula

$$V_{\rm Coul} = Z_L Z_H e^2 / R_s \ , \quad (19)$$

where Z_L and Z_H are the atomic numbers of the lighter and heavier exit fragments, respectively. The neck length parameter d is taken as the only adjustable parameter of the model. Its value is found to be $d = 3.0 \pm 0.5$ fm as is commonly adopted in the literature [7,13,35–37] for the mass region of interest. The large value of d used for the neck mimics the finite-range and diffuse-surface effects [11] of importance for the light-mass systems [38] and, as a consequence, this makes the scission configurations closely resemble the saddle configurations. The other parameters are either fixed (for instance, we use a constant value of $r_s = 1.2$ fm in this work in accordance with previous studies [19,21]) or determined by the measured fusion cross sections (see Sec. III). An alternative and more sophisticated approach to evaluate the transmission coefficients at the scission point is the use of a Krappe-Nix-Sierk [39] potential for $V \ (L = 0)$. Calculations of this kind have been performed for the ^{35}Cl+^{12}C reaction [7,13] at $E_{\rm lab} = 180$ and 200 MeV with very similar results as the ones shown in Fig. 2 with the simplest parametrization. Another study [4] involving a heavier-mass system has shown that the choice of the potential does not provide very different predictions in statistical models.

All other quantities for evaluating the phase-space integrations in Eqs. (12), (13), (14), and (15) are the same as in the case of the light-particle evaporation description. In the actual calculations, the phase-space integrations of Eqs. (12), (13), (14), and (15) are performed with a high precision for the numerical integrations without any approximations. The energy integrations are performed with 1 MeV energy steps and all the values of the cascade decay are stored in 1 MeV steps and $1\hbar$ angular momentum steps.

III. EHFM+CASCADE CALCULATION PROCEDURES

In order to show the basic viewpoint of the EHFM and to demonstrate its applicability for the decay mechanisms of compound nuclei as formed in light heavy-ion reactions, we perform EHFM+CASCADE calculations by introducing very simplified schemes which are presented as follows. In light heavy-ion reactions at moderate incident energies such as the $^{32}S+^{24}Mg$ and $^{35}Cl+^{12}C$ reactions which have been selected as typical examples in this paper, it seems quite reasonable to assume that the second-chance, the third-chance, and many-chance binary decays from the heated daughter nuclei (ER's) populated by light-particle evaporation in the early stages are negligible. Therefore the EHFM is applied to the phase-space calculations only in the first-chance binary decay of complex fragments (i.e., first-chance fissionlike binary decay) from the fused system. Because the complex fragments emitted in the first-chance decay are expected to be populated in the rather highly excited states in both energy and angular momentum in a similar manner to the ER's, the heated fragments including the ER's need to be cooled down until the resulting products are unable to undergo further decay. Therefore the series of these calculations is called EHFM+CASCADE.

From a result of the EHFM+CASCADE calculations physical quantities such as charge-, mass-, and kinetic-energy distributions can be deduced to be compared to experimental observables. For instance, the missing charge and its distributions corresponding to the experimental conditions in coincidence measurements are found to be clearly described with this EHFM+CASCADE calculation. These definitions are found to reasonably well reproduce the experimental distributions as shown in the next section. In the present section, the calculation procedures of EHFM+CASCADE are presented according to the chosen approximations.

The initial conditions required to perform the EHFM +CASCADE calculation are mainly determined by the total fusion cross section $\sigma_{\rm fus}$ which is assumed to be given as the compound nucleus formation with atomic number $Z_{\rm CN}$ and neutron number $N_{\rm CN}$ and at the excitation energy E_x in the heavy-ion reaction under consideration as follows:

$$\sigma_{\rm fus}=\sum_{J=0}^{\infty}\sigma_{\rm fus}(J)=\pi\lambda\!\!\!^{-2}\sum_{J=0}^{\infty}(2J+1)T_{(J)}^{(\rm fus)}, \qquad (20)$$

where $\lambda\!\!\!^{-}$ and J are, respectively, the wavelength and the total angular momentum of the incident channel of the reaction. For the sake of simplicity, the partial wave dependence of the fusion cross section $\sigma_{\rm fus}(J)$ is represented by the transmission coefficient $T_{(J)}^{(\rm fus)}$ with Fermi distribution,

$$T_{(J)}^{(\rm fus)}=\frac{1}{1+\exp[(J-J_{\rm cr})/\Delta_J]}\ . \qquad (21)$$

The critical angular momentum $J_{\rm cr}$ is chosen so as to reproduce the measured complete fusion cross section $\sigma_{\rm fus}$ including both ER and FF yields. Although little is known about the diffuseness parameter Δ_J, its value has been fixed to $1\hbar$ in the present study in accordance with the value usually taken for the transition-state model calculations of Sanders [11] or other evaporation codes [21,22]. The sensitivity of this angular momentum diffuseness parameter has been carefully checked and very small and thus nonsignificant effects have been found on the calculated results.

All the available complex-fragment pairs are introduced in the first-chance decay as part of the binary decay in addition to proton, neutron, and α-particle evaporation (ER's) from the fused system. As discussed in the previous section, the $^{2,3}H$ and ^{3}He evaporation channels are included only in the first-chance decay, whereas the GDR γ-ray emission is also included in the whole CASCADE calculation.

The decay ratio $R_J^{(c)}$ in Eq. (2) is evaluated, as shown previously, for all of the exit channels by using the fusion partial cross section $\sigma_{\rm fus}(J)$ of Eq. (20) as the cross section $\sigma_J(E_x)$ of Eq. (1). During the course of the calculations of the whole phase-space integrations for all decay channels, all the quantities which are needed in the subsequent CASCADE calculations should be stored. However, because of the fact that the memory space of the available computer is not large enough to store the calculated results for all the dependent variables in the first-chance EHFM calculation, the calculated results are stored in the two groups somewhat inclusively as follows. The excitation energy and angular momentum distributions for each fragment with atomic number Z' and neutron number N' are stored in the form of $\sigma_{(Z',N')}(\epsilon',I')$ as a value of cross section and the kinetic-energy distribution of the first-chance emission of fragments is also stored as the form $\sigma_{(Z',N')}(E')$ where E is the kinetic energy of the relative motion between the binary fragments. In order to make the notation clear, in this paper a prime is put on the quantities which correspond to the first-chance EHFM calculations. As has been expected, the distributions $\sigma_{(Z',N')}(\epsilon',I')$ of the fragments with atomic number Z' and neutron number N' obtained in the first-chance decay are in rather highly excited states (for example, see Fig. 3 as discussed in the next section). Then the usual CASCADE calculations are applied to the hot fragments thus populated in the first-chance EHFM calculation.

The final distributions $\sigma_{(Z',N')}(\epsilon,I,Z,N)$ of the fragment with atomic number Z and neutron number N are obtained as the result of the light-particle cascade decay of each fragment with atomic number Z' and neutron number N' which is populated with the cross section $\sigma_{(Z',N')}(\epsilon',I')$ in the first-chance EHFM calculation. In the course of the CASCADE calculation, the distributions $\sigma_{(Z',N')}(\epsilon,I,Z,N)$ can be stored in the computer memory, but due to computer memory limitations the final results are stored in the inclusive form

$$\sigma_{(Z',N')}(Z,N)=\sum_{\epsilon,I}\sigma_{(Z',N')}(\epsilon,I,Z,N)\ . \qquad (22)$$

Then the charge and mass distributions $\sigma(Z)$ and $\sigma(A)$ can be directly compared to experimental data by summing up the final distributions $\sigma_{(Z',N')}(Z,N)$ relative to each the first-chance emitted fragment with atomic number Z' and neutron number N'.

The average velocities of the first-chance emitted fragments are not expected to be greatly modified by the effect of post-scission light-particle cascade decay. The fragment kinetic-energy distributions $\sigma_{(Z',N')}(E')$ which are obtained

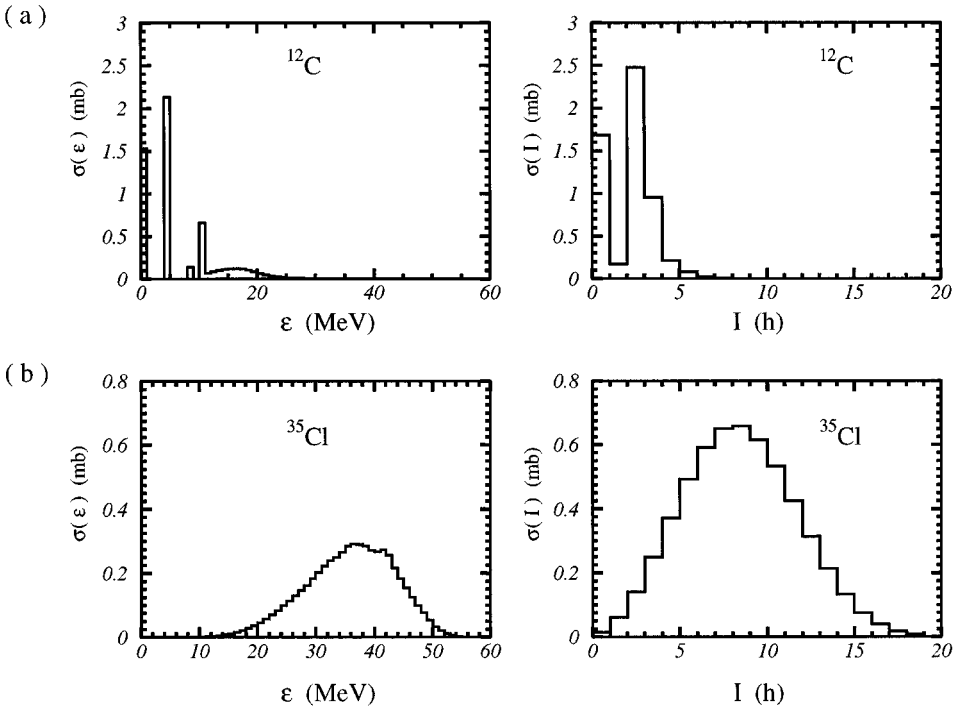

FIG. 3. (a) Internal excitation-energy and angular-momentum distributions of the ^{12}C fragment as obtained by the first-chance EHFM calculations. The distributions of the binary-partner nucleus ^{35}Cl of the ^{12}C fragment are shown in (b) (see text).

in the first-chance EHFM calculation in the center-of-mass system are transformed to kinetic-energy distributions for a given laboratory angle $\theta_{\rm lab}$,

$$\frac{d^2\sigma_{(Z',N')}}{d\Omega_{\rm lab}dE'_{\rm lab}}, \tag{23}$$

by using the usual transformation formula. In this calculation the angular distribution of the fragments of binary decay at the first-chance emission is assumed to have the usual $1/\sin(\theta_{\rm c.m.})$ angle dependence in the center-of-mass system of fissionlike processes.

In order to simplify the notation to define both the missing charge and the kinetic energy distributions in the calculation, the charge distributions $\sigma_{(Z',N')}(Z)$ of the final fragments with the atomic number Z which are populated by the light-particle cascade decay of the hot fragments with atomic number Z and neutron number N are

$$\sigma_{(Z',N')}(Z)=\sum_N \sigma_{(Z',N')}(Z,N)\ , \tag{24}$$

and the probability distributions $P_{(Z',N')}(Z)$ are defined as a function of the charge distributions $\sigma_{(Z',N')}(Z)$ as

$$P_{(Z',N')}(Z)=\frac{\sigma_{(Z',N')}(Z)}{\Sigma_{Z''}\sigma_{(Z',N')}(Z'')}\ . \tag{25}$$

By using the probability distributions $P_{(Z',N')}(Z)$, the kinetic-energy distributions modified by the light-particle cascade decay after scission are evaluated as follows for the fragments with the atomic number Z' and the kinetic energy $E'_{\rm lab}$ which have been obtained in the first-chance EHFM calculation:

$$\frac{d^2\sigma_{(Z)}}{d\Omega_{\rm lab}dE_{\rm lab}}=\sum_{(Z',N')} P_{(Z',N')}(Z)\frac{d^2\sigma_{(Z',N')}}{d\Omega_{\rm lab}dE'_{\rm lab}}\ . \tag{26}$$

Here the relation between kinetic energy $E'_{\rm lab}$ of the first-chance emission and final measured kinetic energy $E_{\rm lab}$ is assumed to be used as follows:

$$E_{\rm lab}=\frac{Z}{Z'}E'_{\rm lab}\ . \tag{27}$$

For the evaluation of the missing charge distribution corresponding to the measured ejectile fragment with atomic number Z_1 in the coincidence measurement (see Ref. [15] for the experimental conditions and results), the coincidence cross sections $\sigma^{(\rm coin)}_{Z_1}(Z_2)$ are defined as follows for the coincident binary partner with atomic number Z_2:

$$\sigma^{(\rm coin)}_{Z_1}(Z_2)=\sum_{(Z'_1,N'_1)} \sigma_{(Z'_1,N'_1)}(Z_1)\sigma_{(Z'_2,N'_2)}(Z_2)\ , \tag{28}$$

where we must keep the condition $Z'_2=Z_{\rm CN}-Z'_1$ and $N'_2=N_{\rm CN}-N'_1$. Then the probability distribution of missing charge for a first fragment with Z_1 is given in the formula

$$P_{(Z_1)}(\Delta Z)=\frac{\sigma^{(\rm coin)}_{(Z_1)}(Z_2)}{\Sigma_{Z''}\sigma^{(\rm coin)}_{(Z_1)}(Z'')}\ , \tag{29}$$

where $\Delta Z=Z_{\rm CN}-(Z_1+Z_2)$ is defined as the missing charge.

Finally the mean values $\langle Z_1+Z_2\rangle$ which correspond to the measured mean charge in coincidence measurements are defined by using the probability distributions $P_{(Z_1)}(\Delta Z)$ of missing charge as follows:

$$\langle Z_1+Z_2\rangle=\sum_{\Delta Z}(Z_1+Z_2)P_{(Z_1)}(\Delta Z)\ . \tag{30}$$

In comparison with other recent statistical-model calculations [6,11], it is worthwhile to mention that one of the main advantages of the present model is the use of a single computer code to follow the whole decay process until all fragments have completely cooled down.

IV. RESULTS AND DISCUSSIONS

Before we present the results of the EHFM+CASCADE calculations which have been performed for a few selected examples, it is important to notice that in this light-mass region it is relevant to use the scission-point approximation of the saddle point. This is due to the fact that both the scission point and the saddle point have geometrical configurations which nearly coincide as recently demonstrated [15] in the case of the binary decay of the ^{47}V system. Alternative available computer codes such as EDCATH [4], GEMINI [5], or EUGENE [40] are essentially based on the saddle-point picture by using the transition-state formalism of Moretto [20] to predict complex-fragment emission yields for heavier systems. The transition-state model developed by Sanders [11] and more specifically adapted for the light-mass region appears to be quite successful by introducing mass-asymmetric fission barriers. On the other hand, the code BUSCO [6] is to our knowledge the only code also following the scission-point approximation with, however [41], the need of the code LILITA [23] to simulate the sequential decay of the binary fragments.

In this section the results of the model will be compared to a number of recently published experimental data [7,11,15,44]. For a more general overview of the experimental systematics of the occurrence of the FF process in the light-mass region previous publications such as Ref. [11] are very helpful.

As pointed out previously in Sec. II one of the most important quantities in the EHFM is the measured ground-state binding energy used to evaluate Q values for the all complex fragments in the phase-space calculations in order to explicitly conserve energy. In order to demonstrate the strong effect of the ground-state binding energy, first of all we choose as a typical example the mass distributions as measured for the ^{32}S+^{24}Mg reaction at two incident energies $E_{\rm lab}$ = 121 and 142 MeV [9] displayed in Figs. 1(a) and 1(b), respectively. It is very interesting to observe that the calculated mass distributions shown by solid histograms reproduce well the characteristic features of the variations from fragment to fragment in the experimental mass distributions shown by open histograms. In these calculations, the critical angular momenta for total fusion cross section at the energies $E_{\rm lab}$ = 121 and 142 MeV are, respectively, $J_{\rm cr}=34\hbar$ and $37\hbar$. These values reproduce the measured complete fusion cross sections which are reported in Ref. [9]. The free parameter d in Eq. (18) which determines the barrier height of the scission point is chosen in this case to be d = 3.5 fm. A systematic investigation of this parameter will be undertaken in a forthcoming publication [33].

In order to understand the reasons why the calculated mass distribution is strongly dependent on the ground-state Q value of the decay fragments, the fragment dependence of the barrier height of the scission point in excitation energy of the compound nucleus for ^{56}Ni is shown in Fig. 1(c). As can be expected in the phase-space integrations P which are shown in Eqs. (12), (13), (14), and (15), the leading term can be evaluated approximately by the form

$$P\sim e^{2\sqrt{a(E_x-V_s)}}\ , \tag{31}$$

where the value of a is equal to the sum of level density parameters of the lighter and heavier fragments in the binary decay. The barrier height V_s of the scission point which is evaluated from the ground state of the CN is given as follows for the case of angular momentum $L=0$:

$$V_s=V_{\rm Coul}+Q\ . \tag{32}$$

In Fig. 1(c) the lowest barrier height of the scission point in the combination of the same mass fragments with different atomic number is plotted. In the case where the lighter fragment is an α-like nucleus its heavy partner is also an α-like nucleus for the ^{56}Ni system; therefore, strong binding energy effects are found in the barrier height of the scission point. It is interesting to note that very similar results are found for the mass fragmentation potential as calculated by Gupta *et al.* [45] for the same system. On the other hand, it has been shown in Ref. [12] that with the use of liquid-drop binding energies the yields do not vary significantly from fragment to fragment. Comparing Figs. 1(a) and 1(b) with Fig. 1(c), the strong enhancements in the measured cross section are well understood as the result of the strong binding energy of α-like fragments.

In the transition-state model calculation [9] the strong binding-energy effect has been taken into account by including Wigner energy terms in the liquid-drop mass formula. Thus the origin of the strong variation from fragment to fragment in the present model may be equivalent to that involved in the transition-state model.

An alternative way to reproduce this strong variation would be to incorporate shell effects in the level density formulas as proposed by Ignatyuk and co-workers [42]. Shell corrections in the energy-dependent (temperature-dependent) a parameter are then produced by the difference of the experimental mass and the liquid-drop mass for each fragment. This possibility will be carefully investigated in the future developments of the EHFM [33]; however, preliminary results on a study of the temperature-dependent level density can be found in the conference proceedings of [43].

Despite of the choice of a very simple parametrization for the present calculations, it should be pointed out that the complete EHFM+CASCADE treatment reproduces well the general trend and also the magnitude of the measured mass distribution. The calculated center-of-mass energy distributions which are obtained in the first-chance emission of the EHFM calculation are found, however, to be a little higher than the measured ones [9] by an amount of about 3 MeV.

In the following we will focus on the case of the ^{35}Cl+^{12}C reaction. The calculated charge distributions in Fig. 2 are compared to the experimental data at $E_{\rm lab}$=180, 200, and 278 MeV, respectively, as obtained in the inclusive measurements [7,13,15,44]. The comparisons are also given for the fissionlike yields for the ^{37}Cl+^{12}C which have been partially

measured at $E_{\rm lab}$=150 MeV [46]. In these calculations the input critical angular momenta $J_{\rm cr}$ were extracted from the total fusion cross section data using the sharp cutoff approximation. Their values are $25\hbar$, $25\hbar$, and $27\hbar$ for the ^{35}Cl incident energies 180, 200, and 278 MeV, respectively. Since the cross section of the complete fusion ER has not been measured for the ^{37}Cl+^{12}C system at $E_{\rm lab}$ = 150 MeV, a $23\hbar$ value was assumed to be the more realistic choice. The value of the d parameter for the barrier height of the scission point is fixed to be d=2.5 fm for each incident energy. It is interesting to observe that this d value is smaller than that in the case of the ^{32}S+^{24}Mg reaction. Although no systematics of the mass dependence of the d parameter for light mass-systems is evident for the moment, it seems that a simple linear dependence with CN fissility might be a reasonable assumption. This possibility will be further quantitatively investigated within the framework of a more systematic study in a forthcoming publication [33].

The charge distributions produced in the first-chance emissions by the EHFM calculations are shown as dashed histograms in Fig. 2 whereas the solid histograms represent the final charge distributions obtained by performing EHFM +CASCADE calculations. In the results of the EHFM calculations as the first-chance decay, we can clearly see the original traces of the binary pairs which are introduced in these calculations as the available decay channels. The cross sections with atomic number Z=20 and 19 arise from the Li and Be emissions, respectively, within a binary-decay process. By comparing the cross sections of complex-fragment binary decays such as B and C emissions, the Li and Be channels have significantly larger cross sections, but these light complex-fragment binary decays do not affect significantly the largest part of the measured charge distributions which comprise the ER's. As expected from the usual Hauser-Feshbach calculations, the cross sections with charge Z=20, 21, and 22 come mainly from the emissions of light particles such as neutrons, protons, and alpha particles. The ^{2,3}H and ^{3}He channels included in the first-chance EHFM calculations are found also to have relatively much smaller contributions in the cross sections for the ER's. Therefore the EHFM+CASCADE calculations for each fragment including the ER's after scission take only neutron, proton, and α-particle emissions into account.

Therefore it can be seen that the results from the EHFM +CASCADE calculations reproduce well the whole measured charge distributions over the entire range of mass asymmetry from the low-mass region of complex-fragment emission (FF) to the heavy-mass region of the evaporation residues (ER's) for all incident energies (see the solid histograms in Fig. 2). Because the measured ground-state binding energies are involved in these calculations also, large yields with α-like fragments are observed for the mass-asymmetric part of the complex-fragment emission. But the heavier partner of the complex-fragment binary decay is not α-like in this system, and then the cross sections with mass-symmetric fragments are not so significant as opposed to the case of the ^{32}S+^{24}Mg reaction presented in previous paragraph.

In the region of the heavier fragments with atomic number larger than about 15, the cross sections are mainly due to the ER's produced by light-particle cascade decays from the compound system. The comparison of the fragments $12<Z<15$ was not possible because their data could not be extracted so accurately from the experiment [15], due to a mixing with both quasi- and deep-inelastic components. It is known, however, that the heavier partners of the complex-fragment binary decay have large cross sections ($\approx$ 10 mb) which correspond to the cross sections of the lighter fragments but the yields are obscured by the considerably larger ER cross sections ($\approx$100 mb for each Z at $E_{\rm lab}$=278 MeV, for example). In the charge region $Z<14$, the complex-fragment emissions become important and essential to reproduce the experimental charge distributions. The light-particle cascade decay of the heavier fragments after scission increases with increasing incident energy. Furthermore, light-particle emissions from the lighter complex fragments after scission are apparent in the case of the highest incident energy $E_{\rm lab}$ = 278 MeV.

At this point it is important to notice that both the predictions of EHFM+CASCADE and the transition-state model [11] provide a quite satisfactory agreement of the general trends of the ^{35}Cl+^{12}C experimental excitation functions over the whole energy range explored as demonstrated in Ref. [15]. This might be a good indication of the validity of the hypothesis that the scission point configurations, as assumed in the present study, almost coincide with the saddle-point shape of the transition-state picture [11].

In order to show how the complex fragments are populated in the excited states at the scission point, the internal excitation energy and angular momentum distributions $\sigma(\epsilon')$ and $\sigma(I')$ of the ^{12}C fragment obtained in the first-chance EHFM calculation in the case of $E_{\rm lab}$=278 MeV are shown in Fig. 3(a). The energy distribution $\sigma(\epsilon')$ is obtained by summing up the angular momentum variable I' of the fragment,

$$\sigma(\epsilon')=\sum_{I'}\sigma_{(Z',N')}(\epsilon',I') \ , \tag{33}$$

and the angular momentum distribution $\sigma(I')$ is also obtained by integrating the internal energy ϵ',

$$\sigma(I')=\int\sigma_{(Z',N')}(\epsilon',I')d\epsilon' \ , \tag{34}$$

where the $\sigma_{(Z',N')}(\epsilon',I')$ is the obtained cross section in the first-chance EHFM calculation (see Sec. III). The distributions of the partner nucleus ^{35}Cl of the ^{12}C fragment in the first-chance emission are shown in Fig. 3(b). As can be understood from Fig. 3(a), the ^{12}C fragment is excited in the lower excited discrete levels, especially the ground 0^+ and first excited 2^+ (4.44 MeV) states. The third large peak corresponds to the 3^- (9.64 MeV) state whereas the smaller one corresponds to the second 0^+ state.

On the other hand, it is clearly seen that the fragment partner ^{35}Cl is statistically excited to the continuous states

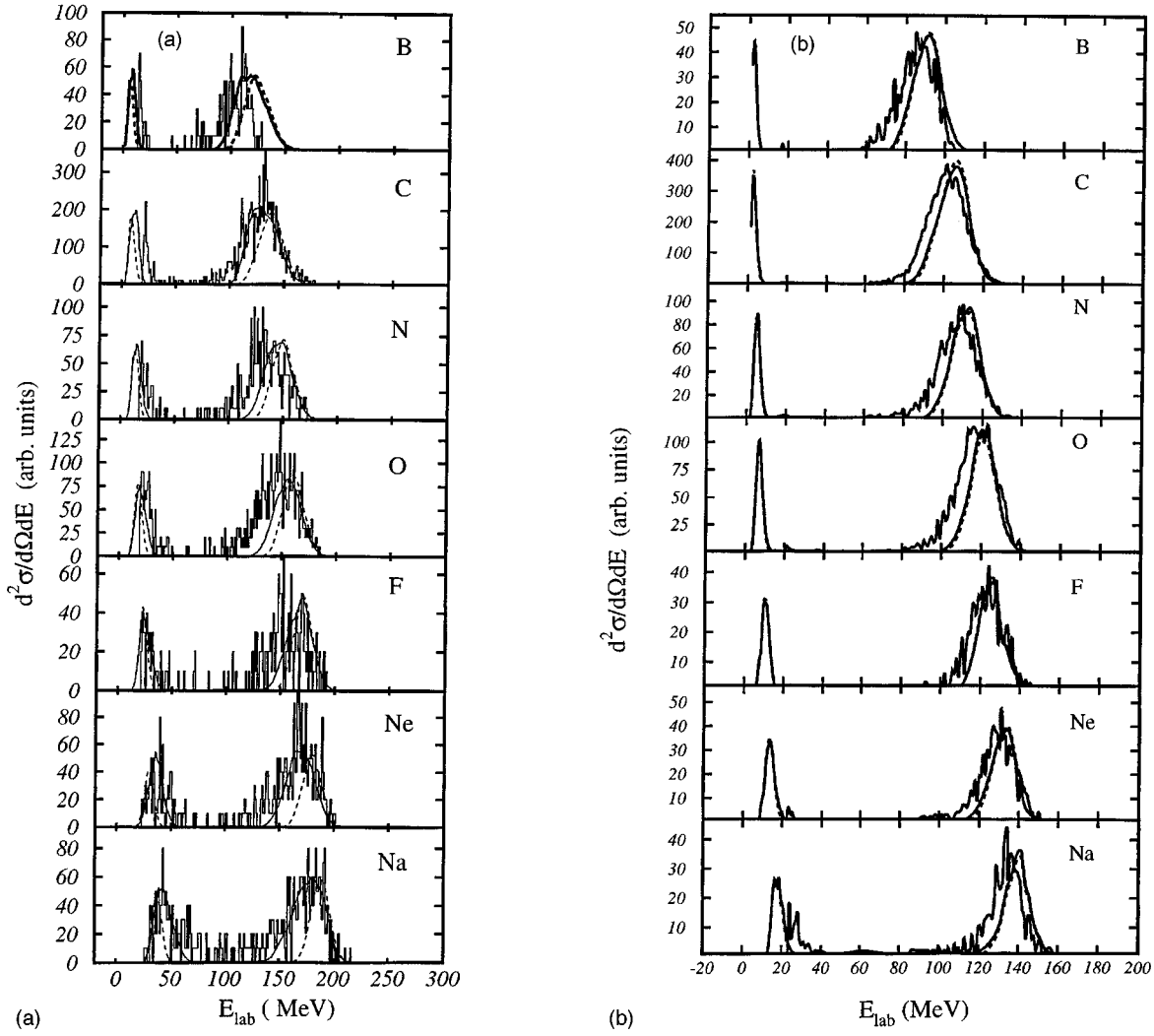

FIG. 4. Comparisons of the experimental inclusive kinetic-energy spectra measured at the laboratory angle $\theta_{lab}=7°$ for each fragments with atomic number from $Z=5$ to $Z=11$ of the $^{35}Cl+^{12}C$ reaction at the incident energies $E_{lab}=278$ MeV (a) and $E_{lab}=180$ MeV (b) with the kinetic energy distributions as obtained with the EHFM and the EHFM+CASCADE calculations. The solid lines are the kinetic-energy distributions evaluated by including the effects of the post-scission light-particle CASCADE decay to the kinetic-energy distributions obtained by the first-chance EHFM calculations shown as dotted lines (see text).

(continuum) with smooth distributions both in internal energy ϵ' and in angular momentum I'. This is a typical behavior of a complex-fragment statistical emission from a equilibrated fused nucleus in the light-mass system region.

At the highest studied incident energy $E_{lab}=278$ MeV, the CN excitation energy of ^{47}V is $E_x=84$ MeV, and the CN lifetime for light-particle emission can be evaluated to correspond to roughly 6×10^{-22} sec by using the standard formula expressed in Eq. (5). As can be seen in Fig. 3(b), on the other hand, the averaged excitation energy of the partner nucleus ^{35}Cl of the ^{12}C fragment is about 35 MeV. The lifetime which corresponds to this excited ^{35}Cl nucleus is about 10 times longer than that of the ^{47}V compound state. Thus we can point out that the proposed picture of light-particle cascade decay after scission of the excited complex fragments obtained in the first-chance EHFM calculation is relevant.

The calculated kinetic-energy distributions of each fragment ($5\leqslant Z\leqslant 11$) in the laboratory system which were evaluated with the procedures outlined in Sec. III are shown in Figs. 4(a) and 4(b) along with the data taken at 7° for two indicated incident energies of $E_{lab}=278$ and 180 MeV, respectively. The dashed lines are the kinetic-energy distributions obtained in the first-chance EHFM calculations and the solid lines are the kinetic-energy distributions including the effect of the light-particle cascade decay after scission. As expected for a so-called inverse kinematics reaction, the kinetic-energy distributions in the laboratory system can be decomposed in two parts: (a) a high-energy component with a typical Gaussian shape which is well measured and (b) a lower-energy component which is deformed by the experimental energy threshold. Therefore it should be taken into consideration that the large deviations from the calculated distributions with the data in the lower-energy parts come from the nonideal experimental conditions.

In the case of the highest measured incident energy $E_{lab}=278$ MeV shown in Fig. 4(a), the effect of the secondary cascade decay of light particles from the hot binary fragments is clear in contrast to the case of the lower incident energy of $E_{lab}=180$ MeV shown in Fig. 4(b) for which the

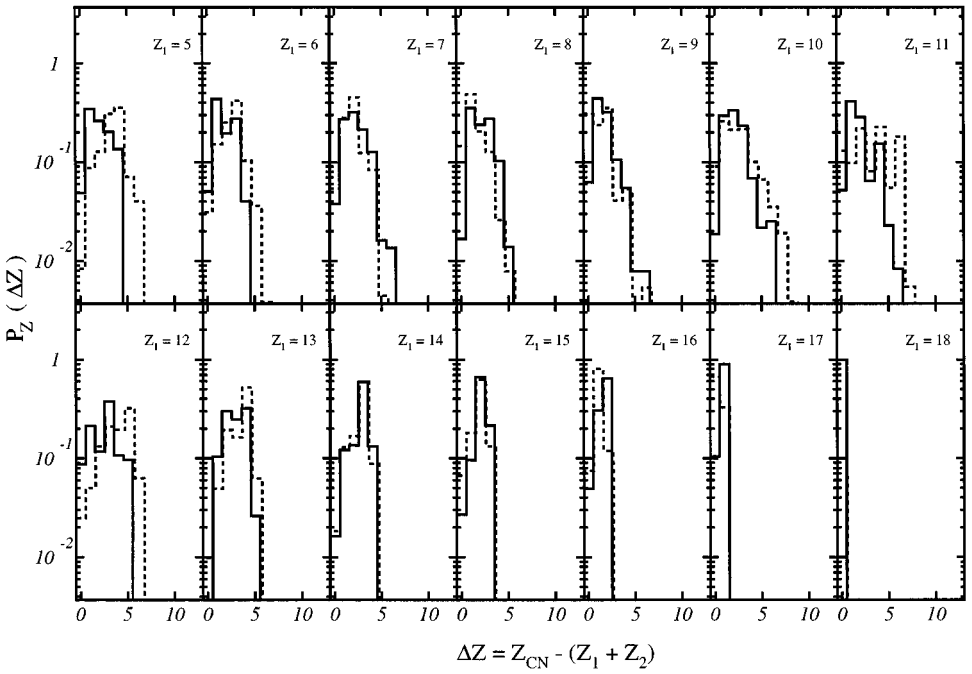

FIG. 5. The missing charge distributions (solid histograms) for the first fragment with atomic number from $Z_1=5$ to $Z_1=18$ as obtained in the coincidence measurements of the ^{35}Cl+^{12}C reaction at $E_{\rm lab}=278$ MeV under the experimental condition of Z_1 and $Z_2\geqslant 5$. The dashed histograms are the calculated values as predicted by EHFM+CASCADE with the same conditions.

differences between the two calculations are not significant. Although for the two calculated kinetic-energy distributions the barrier heights of the scission point which have been used appear slightly larger than the measured ones, the calculations reproduce reasonably well the general trend of the experimental data for both the mean values and the associated widths.

In Fig. 5, the missing charge distributions for the elemental fragments which have been obtained in the coincident data [15], with the experimental conditions of $Z_1\geqslant 5$ and $Z_2\geqslant 5$ with the optimum values of the angular correlations, are shown by the solid histograms. Here the Z_1 is the atomic number of the first fragment and Z_2 the atomic number of its binary partner in the coincidence measurement. The distributions as calculated with EHFM+CASCADE are shown by the dashed histograms for each fragment with atomic number Z_1. The details of these calculations which were adapted to the experimental conditions are given in Sec. III by assuming that the missing charges have their origin from the cascade decay of light particles or binary fragments after scission.

Despite the relative simplicity of the calculations resulting from the direct use of the ground-state binding energy for the full course of the cascade decay without any corrections for the level density parameters, the calculated distributions for each coincident fragment reproduce well the general trend of the experimental results. The large discrepancies observed for $Z_1=5$ might be due to an experimental bias arising from the geometry of detector angles chosen for the coincidence measurements of the angular correlations. A strong α emission in the calculated results is observed for the missing charge distributions of the $Z_1=11$ and 12 binary pair. These deviations should be considered carefully in future studies taking into account the ground-state binding energies directly in the calculations. However, it should be stressed that these calculated missing charge distributions reproduce well the general trends of the experimental ones obtained in the coincidence measurements [15].

Finally we can evaluate the average values of missing charges for the distributions as shown in Fig. 5, which results can be summarized in Fig. 6 by showing how the averaged values depend on the fragments of the coincidence measurements by the use of the mean values $\langle Z_1+Z_2\rangle$. The calculated mean values obtained in EHFM+CASCADE are shown by the solid lines whereas the experimental results are displayed by the data points with their associated error bars for the ^{35}Cl+^{12}C reaction at $E_{\rm lab}=200$ [13] and 278 MeV [15] as a function of the atomic number Z_1 of the first fragment in Figs. 6(a) and 6(b), respectively. As can be seen in the comparisons between the experimental and calculated missing charge distributions, it should be once again stressed that the EFHM+CASCADE calculations reproduce well the general trend of the experimental data.

Knowing that the pre-scission emission of light particles is predicted to be negligible in the model, it can be concluded that the missing charge obtained for the ^{35}Cl+^{12}C reaction in the coincidence measurements for bombarding energies lower than 8 MeV/nucleon has its origin in the light-particle cascade decay of the excited binary fragments after scission. A similar conclusion has been advanced for study of the ^{35}Cl+^{24}Mg reaction measured at $\approx$ 8 MeV/nucleon which preliminary experimental results are also well reproduced by EHFM+CASCADE [47].

V. SUMMARY AND CONCLUSIONS

In order to treat the binary-decay emission of complex fragments in a similar manner to the light-particle evapora-

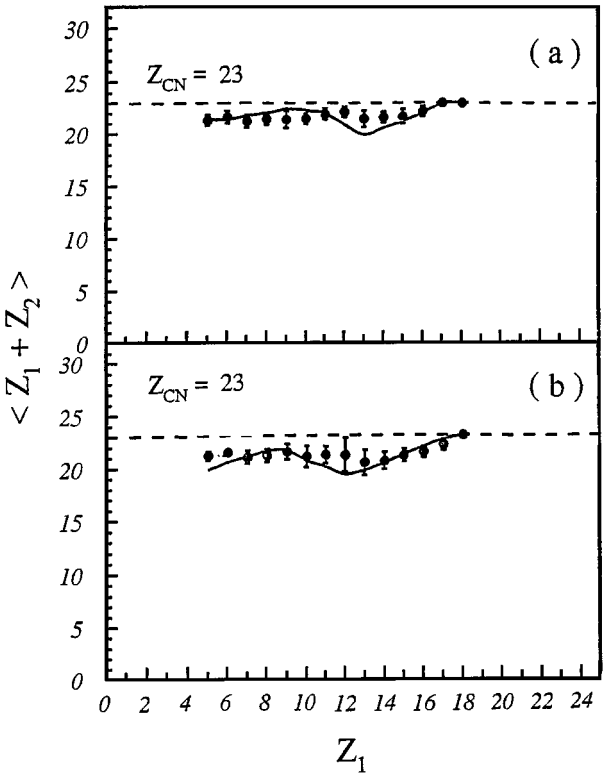

FIG. 6. Comparisons of the mean values $\langle Z_1+Z_2\rangle$ as obtained by the EHFM+CASCADE calculations (solid lines) with the corresponding results of the coincidence measurements for the ^{35}Cl+^{12}C reaction at the incident energies E_{lab}=200 MeV (a) and 278 MeV (b) which are shown as a function of the first fragment's atomic number Z_1. The dashed lines represent the total charge of the compound nucleus Z_{CN}=23.

tion from light-mass compound systems as populated by heavy-ion fusion reactions, the well-known Hauser-Feshbach formalism has been extended in a natural way to the phase-space calculations of the binary decay (i.e., a fusion-fission process) (see Sec. II B). The EHFM calculation is applied to the first-chance binary decay from the compound system by assuming that the second-chance binary decay [from the hot daughter nuclei (ER's) populated by light-particle evaporation in the early stages] is found to be negligible. The internal excitations of the emitted complex fragments are populated in rather highly excited states in both angular momenta and energies in a similar manner to the ER's. The hot binary fragments are cooled down by the cascade of light-particle emissions. Subsequently EHFM+CASCADE calculations can clearly define the physical quantities which are able to be directly compared with the experimental ones such as missing charge distribution (see Sec. III).

The validity of these procedures is shown to be reasonable by referring to the light-particle decay times which are found to have the expected values. In order to make clear how the extension of the statistical model to the emission of complex fragments is relevant, the calculations have been performed within its most simplified version, namely, the parametrization of the barrier height of the scission point with the inclusion of the neck degree of freedom d which mimics the diffuse-surface effects known to be of importance in the light-mass region.

The essential points of the EHFM+CASCADE calculation are presented with the example of the binary decay of the ^{56}Ni nucleus as formed by the ^{32}S+^{24}Mg reaction at two bombarding energies E_{lab}=121 and 142 MeV [9]. The EHFM+CASCADE calculation has also been applied to the ^{47,49}V systems which are formed in the ^{35,37}Cl+^{12}C reactions at E_{lab}=150, 180, 200, and 278 MeV [7,13,15,44,46]. In this case the neck length parameter of Eq. (18) is fixed as d=2.5 fm for all incident energies, whereas its value has been found larger in the case of the ^{56}Ni compound system. As a matter of fact the neck degree of freedom cannot be considered as a simple adjustable parameter since first its value $d=3.0\pm0.5$ fm appears to be strongly constrainted by the size, i.e., the fissility of the compound system and second is non temperature dependent for a chosen reaction. Work is now in progress [33] in order to define a reasonable mass dependence of this parameter through the investigation of new available fusion-fission data on nuclei such as ^{44}Ti [48], ^{48}Cr [16], or ^{59}Cu [47]. The values of the critical angular momenta J_{cr} have been chosen so as to reproduce the measured fusion cross sections. The post-scission light-particle decay of the emitted complex fragments appears to be, in each studied case, of great importance to obtain a reasonably good agreement for all the measured observables: mass-, charge-, and kinetic-energy distributions of both the complex fragments and the ER's. The post-scission light-particle emission is necessary in order to reproduce well the measured missing charge distributions obtained in exclusive fragment-fragment coincidence experiments.

However, many problems still have to be resolved in order to establish the systematic behavior of the fusion-fission process in the light-mass region. The estimate of the barrier height of the scission point has to be more quantitatively investigated although a linear dependence of the neck degree of freedom with the fissility of the compound system seems to be a realistic approximation. Of course the consistent introduction of deformation effects for both ER's and complex fragments has to be considered for the systematic estimation. On the other hand, the direct use of OM transmission coefficients for evaluating the phase-space integration of the complex-fragment binary decay is highly desirable to uncover the more interesting features which are included in the EHFM. Future studies will be undertaken in these directions [33].

ACKNOWLEDGMENTS

The authors wish to thank R.M. Freeman for fruitful discussions and for a careful reading of the manuscript. One of us (C.B.) wishes also to acknowledge S.J. Sanders and Raj K. Gupta for enlightening comments on the model calculations of Refs. [11,45]. A large part of the EHFM+CASCADE calculations has been carried out on the HITACHI-3050RX Work Station at Shinshu University and DEC-osf1 at RIKEN Japan.

[1] L. G. Sobotka, M. A. McMahan, R. J. McDonald, C. Signarbieux, G. J. Wozniak, M. L. Padgett, J. H. Gu, Z. H. Liu, Z. Q. Yao, and L. G. Moretto, Phys. Rev. Lett. **53**, 2004 (1984).

[2] S. J. Sanders, R. R. Betts, I. Ahmad, K. T. Lesko, S. Saini, B. D. Wilkins, F. Videbaek, and B. K. Dichter, Phys. Rev. C **34**, 1746 (1986).

[3] B. Shivakumar, S. Ayik, B. A. Harmon, and D. Shapira, Phys. Rev. C **35**, 1730 (1987); S. Ayik, D. Shapiro, and B. Shivakumar, *ibid.* **38**, 2610 (1988).

[4] F. Auger, B. Berthier, A. Cunsolo, A. Foti, W. Mittig, J. M. Pascaud, E. Plagnol, J. Quebert, and J. P. Wieleczko, Phys. Rev. C **35**, 190 (1987).

[5] R. G. Charity, M. A. McMahan, G. J. Wozniak, R. J. McDonald, L. G. Moretto, D. G. Sarantites, L. G. Sobotka, G. Guarino, A. Pantaleo, L. Fiore, A. Gobbi, and K. D. Hildenbrand, Nucl. Phys. **A483**, 371 (1988).

[6] J. Gomez del Campo, J. L. Charvet, A. D'Onofrio, R. L. Auble, J. R. Beene, M. L. Halbert, and H. J. Kim, Phys. Rev. Lett. **61**, 290 (1988); J. Gomez del Campo, R. L. Auble, J. R. Beene, M. L. Halbert, H. J. Kim, A. D'Onofrio, and J. L. Charvet, Phys. Rev. C **43**, 2689 (1991).

[7] C. Beck, B. Djerroud, F. Haas, R. M. Freeman, A. Hachem, B. Heusch, A. Morsad, M. Youlal, Y. Abe, R. Dayras, J. P. Wieleczko, T. Matsuse, and S. M. Lee, Z. Phys. A **343**, 309 (1992).

[8] K. Yuasa-Nakagawa, Y. H. Pu, S. C. Jeong, T. Mizota, Y. Futami, S. M. Lee, T. Nakagawa, B. Heusch, K. Ieki, and T. Matsuse, Phys. Lett. B **283**, 185 (1992); Y. Futami, K. Yuasa-Nakagawa, T. Nakagawa, S. M. Lee, K. Furutaka, K. Matsuda, K. Yoshida, S. C. Jeong, H. Fujihara, T. Mizota, Y. Honjo, S. Tomita, B. Heusch, K. Ieki, J. Kasagi, W. Q. Shen, and T. Matsuse, Nucl. Phys. **A607**, 85 (1996).

[9] S. J. Sanders, D. G. Kovar, B. B. Back, C. Beck, B. K. Dichter, D. J. Henderson, R. V. F. Janssens, J. G. Keller, S. Kaufman, T.-F. Wang, B. D. Wilkins, and F. Videbaek, Phys. Rev. Lett. **59**, 2856 (1987); S. J. Sanders, D. K. Kovar, B. B. Back, C. Beck, D. J. Henderson, R. V. F. Janssens, T.-F. Wang, and B. D. Wilkins, Phys. Rev. C **40**, 2091 (1989).

[10] A. Ray, D. Shapira, J. Gomez del Campo, H. J. Kim, C. Beck, B. Djerroud, B. Heusch, D. Blumenthal, and B. Shivakumar, Phys. Rev. C **44**, 514 (1991).

[11] S. J. Sanders, Phys. Rev. C **44**, 2676 (1991), and references therein.

[12] T. Matsuse, S. M. Lee, and C. Beck, in *Proceedings of the Symposium on Heavy-Ion Physics and its Application,* Lanzhoo 1990, edited by W. R. Shen, X. Y. Luo, and J. Y. Liu (World Scientific, Singapore, 1991), p. 95; T. Matsuse, S. M. Lee, Y. H. Pu, K. Y. Nakagawa, C. Beck, and T. Nakagawa, in *Towards a Unified Picture of Nuclear Dynamics,* edited by Y. Abe, S. M. Lee, and F. Sakata, AIP Conf. Proc. No. 250 (AIP, New York, 1992).

[13] B. Djerroud, Ph.D. thesis, Strasbourg University, 1992, Report No. CRN/PN 92/32, 1992.

[14] C. Beck, B. Djerroud, F. Haas, R. M. Freeman, A. Hachem, B. Heusch, A. Morsad, M. Vuillet-A-Cilles, and S. J. Sanders, Phys. Rev. C **47**, 2093 (1993).

[15] C. Beck, D. Mahboub, R. Nouicer, T. Matsuse, B. Djerroud, R. M. Freeman, F. Haas, A. Hachem, A. Morsad, M. Youlal, S. J. Sanders, R. Dayras, J. P. Wieleczko, E. Berthoumieux, R. Legrain, E. Pollacco, Sl. Cavallaro, E. De Filippo, G. Lanzanò, A. Pagano, and M. L. Sperduto, Phys. Rev. C **54**, 227 (1996).

[16] K. A. Farrar, S. J. Sanders, A. K. Drummer, A. T. Hasan, F. W. Prosser, B. B. Back, R. Betts, M. P. Carpenter, B. Crowell, M. Freer, D. J. Henderson, R. V. F. Janssens, T. L. Khoo, T. Lauritzen, Y. Liang, D. Nisius, A. H. Wuosmaa, C. Beck, R. M. Freeman, Sl. Cavallaro, and A. Szanto de Toledo, Phys. Rev. C **54**, 1249 (1996).

[17] T. Matsuse, in Proceedings of the International Symposium on Heavy Ion Fusion Reactions, Tsukuba, Japan, 1984, p. 112; S. M. Lee, W. Yokota, and T. Matsuse, in Proceedings of the Many Facets of Heavy-Ion Fusion Reactions, Argonne, 1986, Argonne National Laboratory Report No. ANL-PHY-86-1 (unpublished), p. 63.

[18] W. Hauser and H. Feshbach, Phys. Rev. **87**, 366 (1952).

[19] R. G. Stokstad, in *Treatise on Heavy Ion Science*, edited by A. Bromley (Plenum, New York, 1984), Vol. III.

[20] L. G. Moretto, Nucl. Phys. **A247**, 211 (1975).

[21] F. Pühlhofer, Nucl. Phys. **A280**, 267 (1977).

[22] PACE is a modified version of the code JULIAN described by A. Gavron, Phys. Rev. C **21**, 230 (1980).

[23] J. Gomez del Campo and R. G. Stokstad, LILITA, a Monte Carlo statistical model code, ORNL Report No. TM-7295, 1981.

[24] F. Ajzenberg-Selove, Nucl. Phys. **A460**, 1 (1986); **A475**, 1 (1987); **A490**, 1 (1988); **A506**, 1 (1990); **A523**, 1 (1991).

[25] P. M. Endt, Nucl. Phys. **A521**, 1 (1990), and references therein.

[26] D. R. Chakrabarty, S. Sen, M. Thoennessen, N. Alamanos, P. Paul, R. Schicker, J. Stachel, and J. J. Gaardhoje, Phys. Rev. C **36**, 1886 (1987).

[27] A. H. Wapstra and G. Audi, Nucl. Phys. **A432**, 1 (1985).

[28] A. Bohr and B. R. Mottelson, *Nuclear Structure* (Benjamin, New York, 1969), Vol. 1.

[29] B. Fornal, F. Gramegna, G. Prete, R. Burch, G. D'Erasmo, E. M. Fiore, A. Pantaleo, V. Paticchio, G. Viesti, P. Blasi, M. Cinausero, F. Lucarelli, M. Anghinolfi, P. Corvisiero, M. Taiuti, A. Zucchaitti, P. F. Bortignon, D. Fabris, G. Nebbia, and J. A. Ruiz, Phys. Rev. C **44**, 2588 (1991).

[30] S. Shlomo and J. B. Natowitz, Phys. Rev. C **44**, 2878 (1991).

[31] C. Beck, F. Haas, R. M. Freeman, B. Heusch, J. P. Coffin, G. Guillaume, F. Rami, and P. Wagner, Nucl. Phys. **A442**, 320 (1985).

[32] C. Beck, D. G. Kovar, S. J. Sanders, B. D. Wilkins, D. J. Henderson, R. V. F. Janssens, W. C. Ma, M. F. Vineyard, T. F. Wang, C. F. Maguire, F. W. Prosser, and G. Rosner, Phys. Rev. C **39**, 2202 (1989).

[33] C Beck, T. Matsuse, and R. Nouicer (unpublished).

[34] J. R. Huizenga, A. N. Bekhami, I. M. Govil, W. U. Schröder, and J. Töke, Phys. Rev. C **40**, 668 (1989).

[35] J. R. Natowitz, M. N. Eggers, P. Gonthier, K. Geoffroy, R. Hanus, C. Towsley, and K. Das, Nucl. Phys. **A277**, 477 (1977).

[36] N. Van Sen, R. Darves-Blanc, J. C. Gondrand, and F. Merchez, Phys. Rev. C **27**, 194 (1983).

[37] Y. H. Pu, S. M. Lee, S. C. Jeong, H. Fujiwara, T. Mizota, Y. Futami, T. Nakagawa, H. Ikezoe, and Y. Nagame, Z. Phys. A **353**, 387 (1996).

[38] C. Beck and A. Szanto de Toledo, Phys. Rev. C **53**, 1989 (1996).

[39] H. J. Krappe, J. R. Nix, and A. J. Sierk, Phys. Rev. C **20**, 992 (1979).
[40] D. Durand, Nucl. Phys. **A541**, 266 (1992).
[41] J. Gomez del Campo, D. Shapiro, M. Korolija, H. J. Kim, K. Teh, J. Shea, J. P. Wieleczko, E. Chávez, M. E. Ortiz, A. Dacal, C. Volant, and A. D'Onofrio, Phys. Rev. C **53**, 222 (1996).
[42] A. V. Ignatyuk, G. N. Smirenkin, and A. S. Tishin, Sov. J. Nucl. Phys. **21**, 255 (1975); A. V. Ignatyuk, K. K. Istekov, and G. N. Smirenkin, *ibid.* **29**, 250 (1979); O. D. Grudzevich, A. V. Ignatyuk, V. I. Plyaskin, and A. V. Zelenetsky, in Proceedings of the International Conference on Nuclear Data for Science and Technology, Mito, Japan, 1988 (unpublished), p. 767.
[43] T. Matsuse and S. M. Lee, in Proceedings of the International Conference on Nuclear Data for Science and Technology, Mito, Japan, 1988 (unpublished), p. 699.
[44] C. Beck, B. Djerroud, B. Heusch, R. Dayras, R. M. Freeman, F. Haas, J. P. Wieleczko, and M. Youlal, Z. Phys. A **334**, 521 (1989).
[45] R. K. Gupta, M. Münchow, A. Sandulescu, and W. Scheid, J. Phys. G **10**, 209 (1984); D. R. Sahora, N. Malhotra, and R. K. Gupta, *ibid.* **11**, L27 (1985); S. S. Malik and R. K. Gupta, *ibid.* **12**, L161 (1986).
[46] W. Yokota, T. Nakagawa, M. Ogihara, T. Komatsubara, Y. Fukuchi, K. Suzuki, W. Galster, Y. Nagashima, K. Furuno, S. M. Lee, T. Mikumo, K. Ideno, Y. Tomita, H. Ikezoe, Y. Sugiyama, and S. Hanashima, Z. Phys. A **333**, 379 (1989).
[47] R. Nouicer, C. Beck, D. Mahboub, T. Matsuse, B. Djerroud, R. M. Freeman, A. Hachem, Sl. Cavallaro, E. De Filippo, G. Lanzanò, A. Pagano, M. L. Sperduto, R. Dayras, E. Berthoumieux, R. Legrain, and E. Pollacco, Z. Phys. A **356**, 5 (1996).
[48] J. M. Oliveira, Jr., *et al.*, Phys. Rev. C **53**, 2926 (1996).